Investigating Correlations between Snowmelt and Forest Fires in a High Latitude Snowmelt Dominated Drainage Basin

KATHRYN A. SEMMENS[1] AND JOAN M. RAMAGE[2]

ABSTRACT

High latitude drainage basins are experiencing increases in temperature higher than the global average with snowmelt dominated basins most sensitive to effects in winter due to snowpack's integration of these changes over the season. This may influence the timing of snowmelt onset, the melt-refreeze period, and snowpack accumulation resulting in changes in spring runoff, associated flooding, and drought conditions later in the year, possibly enhancing forest fire potential. Large burned areas cleared of vegetation change discharge dynamics and may affect snowmelt characteristics in subsequent seasons. Correlations are tested by comparing forest fire occurrence with spring melt onset, the end of melt-refreeze period (after which snow rapidly depletes) and early snowmelt events. Snow characteristics are derived from brightness temperature (T_b) data from the Advanced Microwave Scanning Radiometer for EOS (AMSR-E) for 2004−2007. Dates of melt onset, end of melt-refreeze, and melt events are defined with T_b and diurnal amplitude variation thresholds. Areas and intensities of forest fires are from MODIS thermal anomaly data (MOD14) and all data are mapped to an EASE-grid to assess spatial correlations. Analysis of high (2004−2005) and low (2006−2007) fire years in the Porcupine sub-basin of the Yukon River in northeastern Alaska and the Yukon Territory show earlier melt onset and end of melt-refreeze in years and areas of high forest fire occurrence. The burned areas also correlate with later melt onset and later end of melt-refreeze in subsequent low fire years.

Keywords: snowmelt, forest fire, melt onset, AMSR-E, brightness temperature

INTRODUCTION

For the past several decades boreal ecosystems in Alaska and Canada have experienced an increase in temperature (1°C over the last 55 years for interior Alaska (Wendler *et al*., 2010)), as well as a doubling of area burned by wildfires and an amplification in frequency of large fire years (Stocks *et al*., 2002; Gillett *et al*., 2004; Kasischke and Turetsky, 2006; Kasischke *et al*., 2010). An increase in extreme fire events has also occurred and late season burning has quadrupled (Kasischke *et al*., 2010). These trends are expected to continue with some estimates of annual burned area increasing 200-300% in the next century with significant implications for carbon storage and losses (Balshi *et al*., 2009; Turetsky *et al*., 2011). Such projected changes also affect ecosystem structure and forest composition (Shenoy *et al*., 2011), permafrost degradation, and water and air quality due to the creation of black carbon aerosols that deposit on snow surfaces, enhancing melting and reducing surface albedo (Randerson *et al*., 2006). Wildfires can affect snow accumulation and melting, alter soil characteristics (especially repellency), and result in more over-

[1] Lehigh University, Earth and Environmental Sciences Department, 1 West Packer Ave., Bethlehem, PA 18015, kas409@lehigh.edu

[2] Lehigh University, Earth and Environmental Sciences Department, 1 West Packer Ave., Bethlehem, PA 18015, ramage@lehigh.edu

land flow, soil distribution and increased discharge (Shakesby and Doerr, 2006). Additionally, in black spruce forests of interior Alaska, fire removal of overstory canopy leads to increased snow exposure and changes in surface energy budgets that persist for years after the fire (Randerson *et al*., 2006).

Annual forest fire occurrence and burned area for Alaska have been recorded since the 1950s. These data suggest there is high variability in area burned, fluctuating from high fire years (average of 66 fires greater than 400 ha) to low fire years (average of 17 fires per year greater than 400 ha) with most fires occurring in the interior of the state, at elevations less than 1000 m a.s.l, and during the six weeks between June and mid-July (Kasischke *et al*., 2002). There is generally a fire season starting in mid June that is driven by thunderstorms and convective activity and a late spring fire season after snowmelt when there is a plethora of dry vegetative fuel and low precipitation (Kasischke *et al*., 2006). Most fires originate as lightning strikes. Fire cycle, defined as the number of years needed to burn the area of interest, increases with elevation due to forest production decreasing with elevation (Kasischke *et al*., 2002). Short fire cycles of less than 120 years are noted in the Yukon/Old Crow Basin ecoregion, the area of interest to this study, which is also characterized by relatively lower average annual precipitation (19.1 cm), relatively higher average lightning strikes (4.9 per 10 ×10 km^2 per year), and 90% tree cover (Kasischke *et al*., 2002).

The Yukon/Old Crow Basin ecoregion is part of the Porcupine River sub-basin (Figure 1), the northeastern 61,400 km^2 portion of the Yukon River basin which drains 853,300 km^2 crossing from northwestern Canada through central Alaska. The sub-basin is characterized by a subarctic nival regime with snowmelt driving runoff that is generally highest from May to September with very low winter flows (Brabets *et al*., 2000). The basin has relatively low relief, is underlain by continuous permafrost and predominately covered with needleleaf forest (Brabets and Long, 2002). Forest fires have a significant impact in permafrost areas, causing long term near-surface permafrost degradation, active layer deepening, and slow forest regeneration (Burn, 1998). The dominant forest land cover, snowmelt driven runoff, and the projected future increase in burned area are the primary reasons for studying fire and snow dynamics in this basin. Additionally, the Yukon/Old Crow Basin has experienced a decrease in fire return interval from 107 (1950−1999) to 92 (1950−2009) reflecting the increase in fire frequency and area burned (Kasischke *et al*., 2010).

Many studies have investigated the causes, characteristics and effects of fires on the ecology and soil in the boreal forest. Here, remote sensing data is utilized to investigate snowmelt and how its timing correlates to years of high and low fires due to similar climatic effects on both snowmelt and forest fire potential. Earlier snowmelt may be indicative of warmer winter temperatures, and an earlier end to the melt-refreeze period may lead to drought conditions in the summer due to depletion of a primary source of moisture. Furthermore, snow behaves differently in open and forested environments with accumulation under dense canopies being relatively smaller due to snow interception and sublimation (Pomeroy *et al*., 2002), so it stands to reason that melt characteristics vary in burned areas, a hybrid of open and forested environments. We hypothesize that snowmelt onset and duration will vary significantly before and after fire seasons in burn areas and test this hypothesis by comparing snowmelt timing parameters for burned versus non-burned areas as well as comparing high versus low fire years. Related is our secondary hypothesis that snowmelt runoff will vary between fire years with earlier and higher peak discharges after high fire years due to increased overland flow. This research will address whether there tends to be earlier melt onset and end of melt-refreeze period for locations that experience significant forest fires, suggesting potential utility for fire season forecasting as well as modeling of snowmelt runoff.

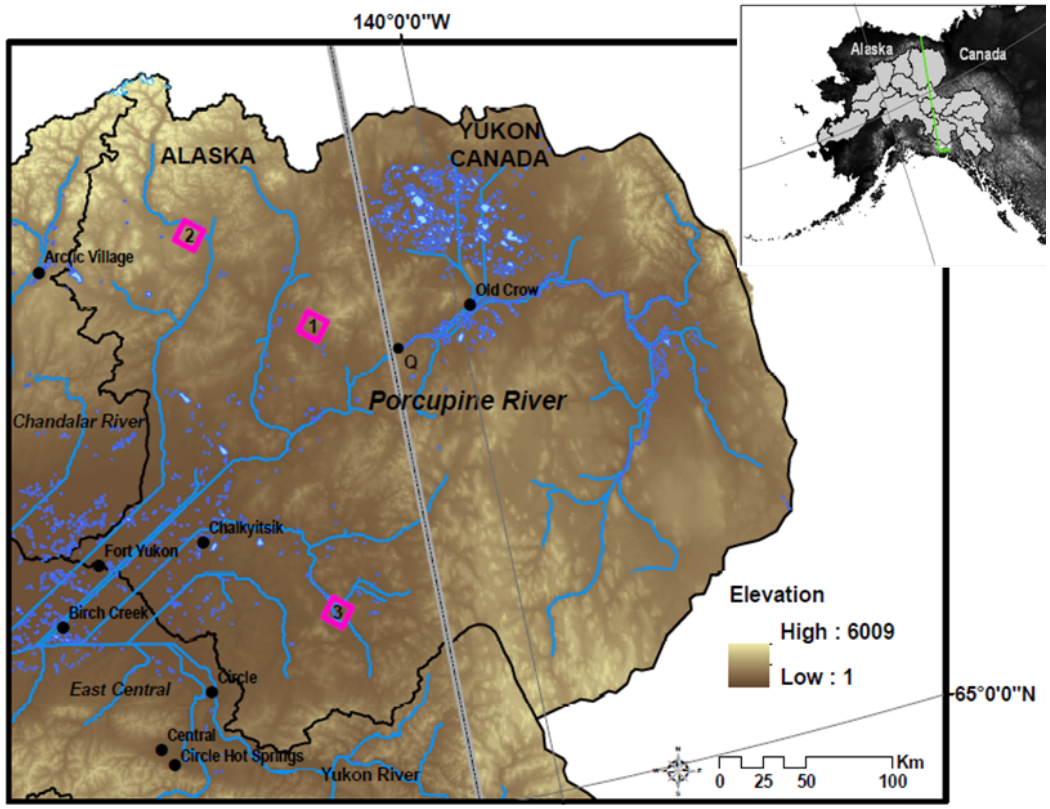

Figure 1. Digital Elevation Model of the Porcupine River Basin. Black circle with symbol Q is the gauge Porcupine at International Border (67°25'27"N, 140°53'28"W), gross drainage area of 59,800 km^2) used in the hydrometric analysis. Pink squares are pixels referenced in results section. Elevation is in meters.

DATA AND METHODS

To investigate correlations between forest fire occurrence and melt timing characteristics, melt onset date, end of melt-refreeze date, and the number of early snowmelt events for both burned and non-burned areas are compared both within and between years from 2004 to 2007. A variety of data sources and techniques are utilized (Table 1).

Table 1 List of data used, their frequency, time series, resolution, and source

Data				
	Frequency/ Wavelength	Date	Spatial Res-olution	Data Sources
AMSR-E L2A Brightness Temperature	36.5 GHz (Vpol)	2004−2007	12.5 km	NSIDC
MODIS MCD14ML Collection 5 (MOD14 Terra/ MYD14 Aqua Active Fire)	1.9 and 11 μm (band 21 and 31)	2004−2007	1 km	NASA USDA-RSAC
Hydrometric data Porcupine River @ Int'l Boundary (67°25'27"N, 140°53'28"W, 59,800 km^2 drainage area)	-	1987−2009	-	Env. Canada
Meteorological data Old Crow Airport (67°34'12"N, 139°50'24"W, 251.2 m elevation)	-	2004−2007	-	Env. Canada

Snow melt timing is derived from brightness temperature (T_b) data from the Advanced Microwave Scanning Radiometer-Earth Observing System (AMSR-E) on the NASA Earth Observing System Aqua satellite (Ashcroft and Wentz, 2006). Fire date, extent, and radiative power (measured in megawatts, MW) are from Moderate Resolution Imaging Spectroradiometer (MODIS) thermal anomaly data (MOD14 Active Fire Product) (USDA, 2010). The fire detection points are accurate to ±50 m and represent the centroid of a 1 km cell where the fire occurred. Air temperature, snow, and precipitation totals from Old Crow Airport in the middle part of the basin are used for validation and hydrometric data from the Porcupine River gauge at the International Boundary are used to assess trends in discharge.

Melting snow is detectable by AMSR-E brightness temperature (T_b) because the presence of liquid water within a snowpack increases its emissivity, thus increasing T_b which is a function of the surface temperature (T_s) and emissivity (E) of the material ($T_b = ET_s$). Therefore there is a significant difference in T_b between wet (emits close to that of a blackbody) and dry snow (Chang *et al*., 1975; Ulaby *et al*., 1986). The 36.5 GHz vertically polarized wavelength is used due to its high sensitivity to water in the snowpack (Ramage *et al*., 2006). AMSR-E has a 14×8 km^2 resolution at 36.5 GHz frequency and has overpass times of 3:30 and 13:30 PST, thus improving on the previously used SSM/I with a higher spatial resolution. SSM/I data and the technique for detecting snowmelt timing has been previously established in the upper Yukon River basin using 37GHz vertically polarized (Ramage *et al.,* 2006) and has been found to correlate well with AMSR-E derived snowmelt onset (Apgar *et al*., 2007).

AMSR-E generally has more than two observations per day in arctic and subarctic regions, and up to eight observations near the poles, allowing diurnal variations to be detected. After averaging T_b 36.5V GHz values that are less than 2.5 h apart, the running difference between two daily (ascending and descending) observations is used to calculate the diurnal amplitude variations (DAV) (Apgar *et al*., 2007). High DAV values, especially for 37 GHz sensitive to the top centimeter of snowpack, indicate when the snowpack is melting during the day and re-freezing at night (Ramage *et al.,* 2006). Previous studies have shown that snow cover distribution and snowmelt timing can be adequately measured by passive microwave sensors daily, in all weather conditions (e.g. Hall *et al*., 1991; Ramage *et al*., 2006). Snowmelt onset is determined from AMSR-E data (36.5 GHz vertically polarized) when T_b is greater than 252 K and DAV are above ±18 K, thresholds previously developed and validated (Apgar *et al*., 2007).

For this analysis, melt onset (and end high DAV) are defined as the first (and last) date when at least three of five consecutive days meet the T_b and DAV thresholds described above. This three of five day algorithm has proven accurate in preliminary results thus far based on manual cross checking of observations and correspondence with estimates from earlier work, but further refinement may be necessary. Previous use of the T_b methods described assumed no significant winter melt periods (Ramage *et al*., 2006). However, early snowmelt events (EMEs), short-lived melt occurrences before melt onset, may be a factor in melt dynamics. These early events are defined here as short melt periods where T_b and DAV are above their thresholds for less than three out of five consecutive days, meaning that melt occurs but is not sustained. The algorithm is constrained to before the melt onset date previously determined. Once melt recurs for more than three successive days, it is deemed melt onset. All derived data are gridded as 12.5 km pixels in NSIDC Ease-Grid.

It is important to note that there are some limitations and sources of error for this approach including the coarse resolution of the AMSR-E data which make it difficult to precisely estimate snow distribution. Additionally, these methods assume the terrain is relatively homogeneous and the snowmelt signal is not distorted by land cover and topography.

RESULTS

Differences between fire years for an area that was burned are apparent in Figure 2, showing T_b and DAV values for pixel 3 (see pink boxes in Figure 1) which burned in 2005 but not 2006. The fire year (2005) has a higher brightness temperature signal in the winter months, an earlier melt onset and earlier end of high DAV/melt-refreeze period, and a slightly longer melt duration (23 days versus 16 days in 2006). The non-fire year (2006) also has higher sustained DAV variations

that begin later in the season compared to 2005. The earlier melt onset and end of melt-refreeze indicate higher winter temperatures and may have contributed to dry conditions in summer due to the earlier depletion of the snowpack as a source of moisture.

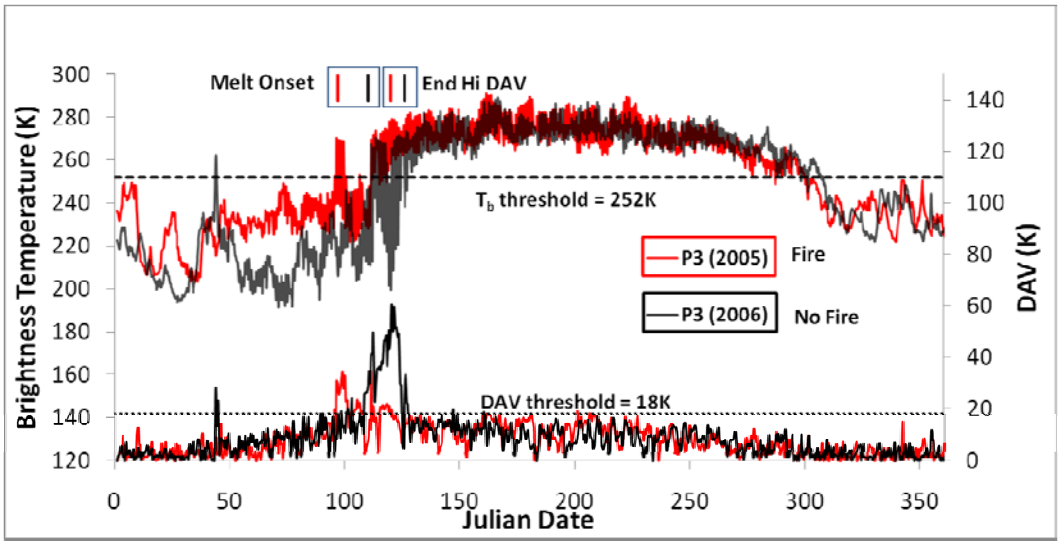

Figure 2. Brightness temperatures (T_b) and diurnal amplitude variation (DAV) for a high fire year (2005) and low fire year (2006) for pixel 3 (average elevation of 259 m) in the Porcupine River basin. Thresholds for T_b and DAV determine melt onset (in Julian dates) when they are met three out of five consecutive days.

Figure 3 further illustrates the differences between burned and unburned pixels with intra-year comparisons. P1 was completed burned in 2005 while P2 was not and both pixels were unburned in 2007. P1 and P2 have mean elevations of 530 and 723 m, respectively. The frequency of T_b values shows higher minimum values for P1 than P2 during 2005 (the high fire year), and more similar distributions in a low fire year (2007). This demonstrates that burned areas vary considerably from unburned areas in high fire years with higher T_b values for the duration of the winter period. Snow accumulation differences could account for some of this difference in distribution. Melt onset dates also reflect these differences between the pixels in the fire year with P1 having the earlier melt onset than P2 (108 versus 116, respectively) while in the non-fire year melt onset is not significantly different (P1 date of 113 compared to P2 date of 115).

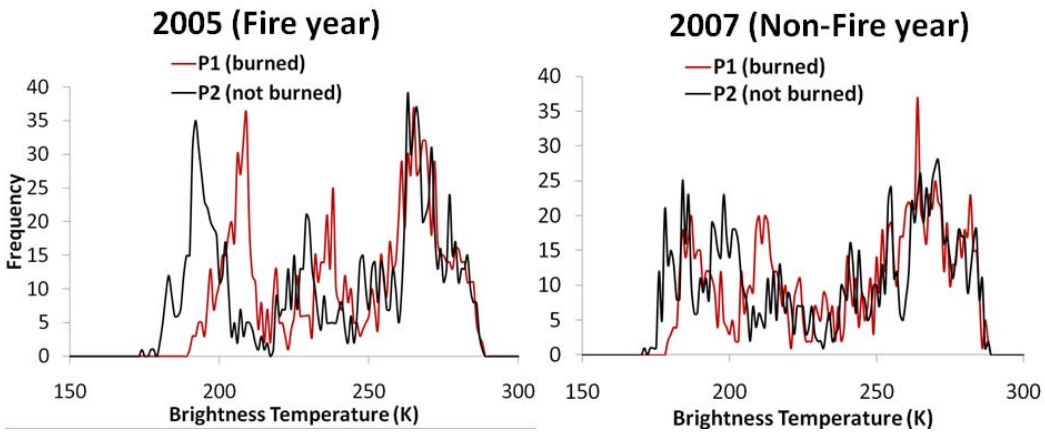

Figure 3. Frequency distribution of brightness temperatures compared for a burned (P1) and unburned (P2) pixel for a high (2005) and low (2007) fire year. The burned pixel has a higher minimum T_b than the unburned in the high fire year (2005) while the two pixels are more similar in the low fire year (2007).

Analysis of variations between burned and unburned areas was extended to the whole basin and average melt onset date (MOD), average end of high DAV date (EHD) and average number of early snowmelt days (EME) compared (Table 2). For all years, the average number of early melt events was not significantly different between fire and non-fire pixels. For the high fire years 2004 and 2005 both average melt onset date and average end of high DAV date were significantly different (p-value <0.00001) between fire and non-fire pixels. In contrast, low fire years were not significantly different between fire and non-fire pixels, possibly a result of lower intensity fires.

Table 2 Average melt onset date (MOD), end of high DAV/melt-refreeze period (EHD), and number of early snowmelt events (EME) for years 2004-2007. Statistical significance from t-test. Calculated burned area for the whole Porcupine River basin is in the first column below year and is derived from a fire perimeter shapefile from the Alaska Interagency Coordination Center. MOD and EHD values are Julian date. EME values are days

Year	Pixel	Avg MOD (Julian Date)	Avg EHD (Julian Date)	Avg EME (# days)	P-value MOD	P-value EHD	P-value EME
2004	Fire	108	124	3.7	<0.00001	<0.00001	0.33
3,860 km^2	Non-fire	118	133	3.8			
2005	Fire	109	120	2.8	<0.00001	<0.00001	0.03
4,010 km^2	Non-fire	114	129	2.4			
2006	Fire	118	131	2.3	0.29	0.02	0.28
165 km^2	Non-fire	119	135	2.6			
2007	Fire	109	126	3	0.1	0.001	0.15
300 km^2	Non-fire	113	135	2.7			

The fire intensity was greater for the high fire years 2004 and 2005 as indicated by a higher fire radiative power and larger extent of burned areas in the Porcupine River basin (Figure 4; Table 2).

Daily discharge (measured in m^3/s at the Porcupine Gauge at International Boundary) was also significantly different during the time period of analysis (Figure 4). In 2006, after the year of most intense fires, discharge peaked earlier and higher than average. In 2005, after the extensive 2004 fires, discharge peaked significantly earlier than average. In contrast, in 2007, after relatively low fire occurrence and power, discharge was markedly reduced and close to the mean (1987-2009). The finding of an increase in peak streamflow after significant fire and burned extent is not surprising and has been found in several other studies (Shakesby and Doerr, 2006; Seibert *et al*., 2010). Fire clears vegetation and seals the soil creating substantial overland flow. While the gauge used is not directly downstream from the majority of the fire activity, it had the most data continuity and is assumed to be a reasonable proxy given that similar increases in peak discharge after fire occurrence are seen in stage height at the Yukon River near Fort Yukon gauge farther downstream (not shown).

Meteorological data at Old Crow, upstream of the gauge show precipitation (snow and rain), snow accumulated on the ground, and fire radiative power over the year for 2003-2005 (2006-2007 did not have enough data for analysis) (Figure 5). There was substantially more rain during the year of low fire radiative power (2003) and the snowpack persisted longer compared to 2004 and 2005, years of high fire radiative power. The amount of snow accumulated is comparatively lower in 2003. However, these measurements are for a single location and are not representative of the spatial variation throughout the basin, while the fire radiative power is for the whole basin. Future work will investigate basinwide accumulation of snow water equivalent (SWE) with estimates from AMSR-E as well as basinwide precipitation (rain and snow) estimates from European Centre for Medium Range Weather Forecasts (ECWMF) ERA-interim re-analysis climate data (Berrisford *et al*., 2009) in order to have a better spatial representation of these parameters.

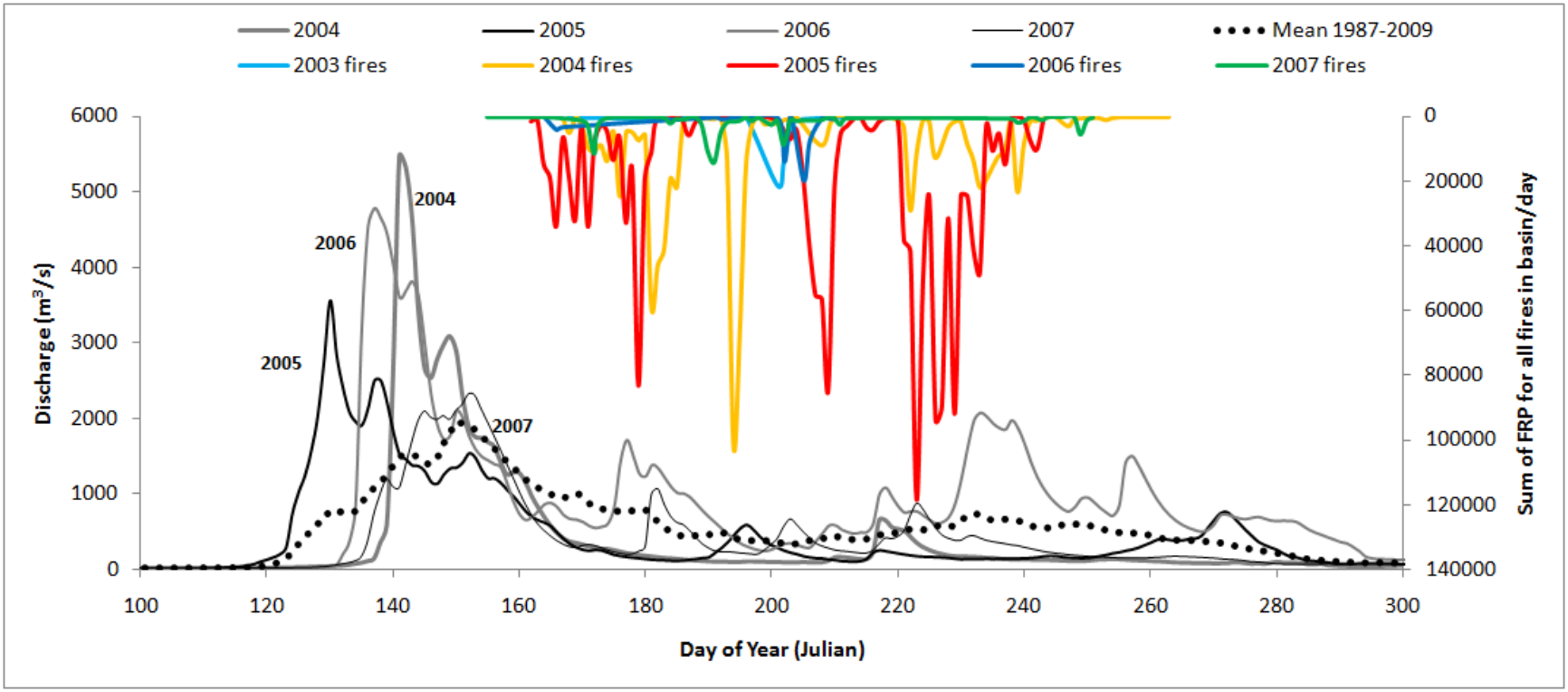

Figure 4. Daily discharge at the Porcupine River gauge at the International Boundary (point Q in figure 1) for 2004 to 2007. Mean flow for the 1987 to 2009 period is shown with dotted line. Cumulative fire radiative power (megawatts) of all fires in the Porcupine basin per date are shown at top (with scale increasing down). Fire radiative power is from MODIS active fire products for years 2003−2007. 2003, 2006, and 2007 were years of lower fire radiative power throughout the basin.

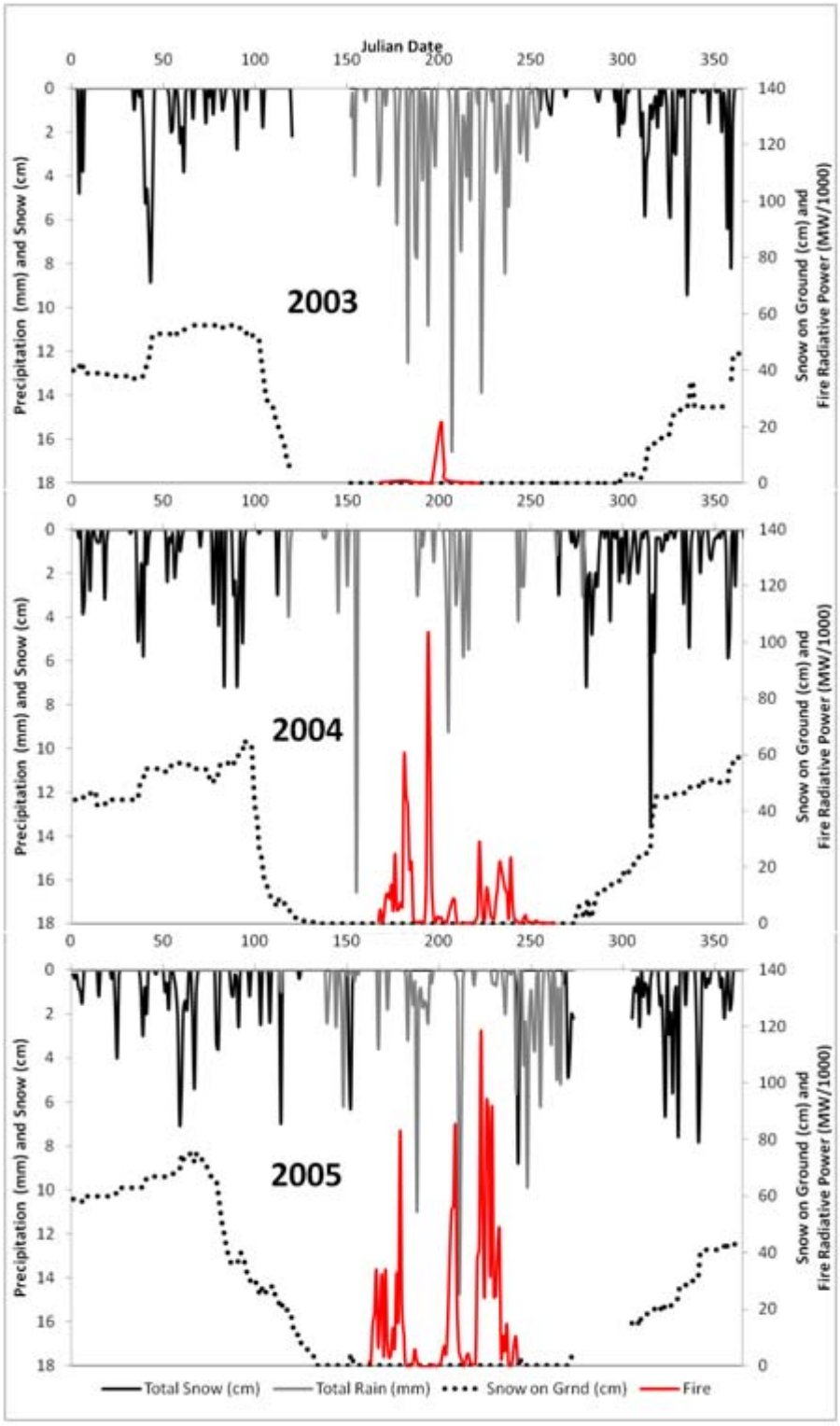

Figure 5. Daily precipitation (mm) and snow (cm) plotted on left axis and accumulated snow on the ground (cm) plotted on the right axis from the Old Crow Airport Station in the Porcupine River sub-basin (67°34'12"N, 139°50'24"W, elevation 251.2 m). Fire radiative power in Megawatts/1000 plotted on the right axis is from MODIS active fire product.

Timing and difference maps of melt onset and end of high DAV (melt-refreeze period) in the Porcupine River basin for the years 2004 to 2007 suggest consistent trends and differences between burned and non-burned areas and high and low fire years. Melt onset maps (Figure 6) show the spatial correlations between earlier melt onset and areas that burn the following summer season. For instance, in 2004 and 2005 over half of the intense, large fires occured in areas that had earlier melt onset. Difference maps of melt onset suggest there is generally later melt onset in burned area pixels the year following the fires, reflecting the previous year's anomalous early onset. The blue colors in and around fire perimeters in the right column of Figure 6 illustrate this. For instance, in 2005 substantial areas experienced fires throughout the basin and the following year (2006) had later melt onset in the majority of the basin. In 2006 there were minimal fire occurrences and relatively later melt onset compared to previous high fire years. In 2007 there were many smaller fires spread throughout the basin and melt onset was earlier throughout the basin; the difference compared to 2006 is seen in the predominantly red difference map.

Similar trends and spatial patterns are evidenced in the difference in the end of the melt-refreeze period (Figure 7), perhaps a more important characteristic pertaining to the fire season due to its indication of timing and duration of moisture content in the landscape. Earlier end of high DAV is evidenced in areas that end up burning during the summer. Subsequent years of lower fire activity are correspondingly later due to the anomalous early end in the fire years (see 2005-2006 difference map). The 2004−2005 difference map shows 2005 to be even earlier in end of melt-refreeze than 2004, possibly a result of cumulative effects of having high fire years back to back or reflecting the higher radiative fire power of the 2005 fires. As in Figure 6, 2007 shows earlier end of high DAV, possibly due to more widespread but lower intensity fires, or due to higher mean ambient winter temperatures compared to other years. Spatial distributions and differences for early snowmelt events (not shown) were more spatially variable with weak correlations between melt days and fire occurrence (Table 2).

DISCUSSION

Wildfire in high latitude boreal ecosystems has far reaching effects from changes to soil characteristics, increases in overland flow, changes in species distribution and abundance, changes in surface energy budgets, alterations of snow accumulation and melt timing, changes in permafrost extent, and contribution of carbon dioxide to the atmosphere. Results from comparison of burned versus unburned pixels for the Porcupine River basin suggest there are significant differences both between the pixels in the fire year and between years for burned pixels. Melt onset and end of melt-refreeze tends to occur earlier in pixels where forest fires occur the following summer season and winter brightness temperatures are higher in high fire years compared to low fire years. Consequently, the difference in a following low fire year is towards later melt onset and melt-refreeze providing further evidence of the anomalous earlier melt onset and end melt-refreeze preceding the fires. Additionally, differences in peak discharge corresponded to high and low fire occurrence, a hydrologic response that was expected. Seibert *et al*. (2010) modeled streamflow using a change detection approach based on pre-fire conditions and parameters and found that observed post-fire flow was 120% higher than expected. An analogous change detection modeling approach could be utilized in future work, assessing expected melt timing versus observed to determine the ecosystem's response before and after fire occurrence.

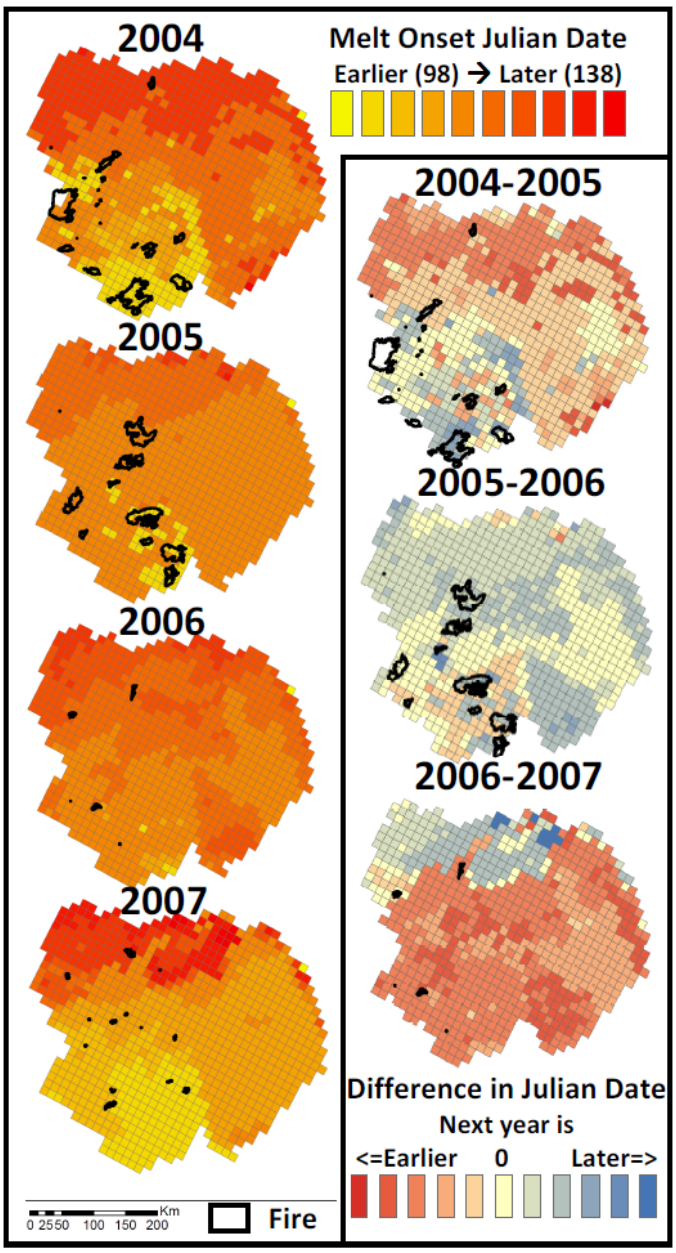

Figure 6. Time series color maps of melt onset for 2004-2007 (left column) and difference maps of melt onset (right column) for the Porcupine River basin (see figure 1 for location). Units are Julian date. Yellow/light orange corresponds to earlier date; bright red is a later melt onset date. For difference maps, red indicates the next year's melt onset was earlier; blue was later. Burned areas are outlined in black.

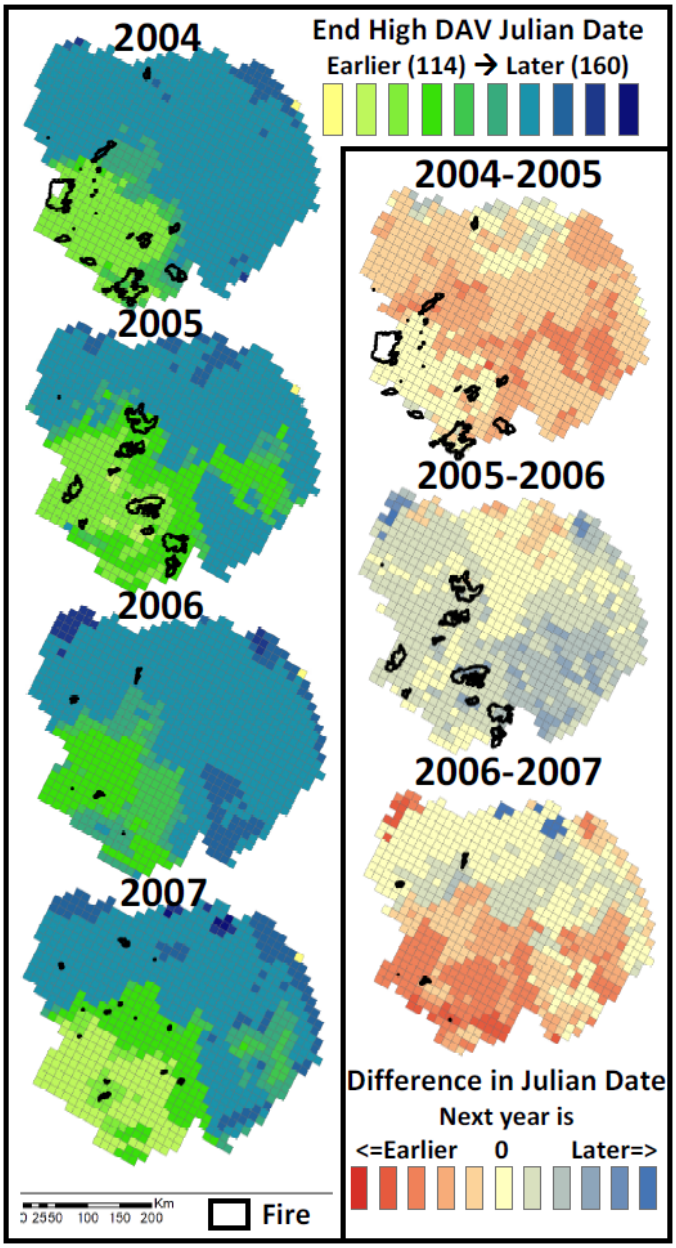

Figure 7. Time series color maps of end high DAV or melt-refreeze period for 2004-2007 (left column) and difference maps of melt onset (right column) for the Porcupine River basin. Units are Julian date. Yellow/light green corresponds to earlier end of melt-refreeze; blue is a later end date. For difference maps, red indicates the next year's end of melt-refreeze was earlier; blue was later. Burned areas are outlined black.

While the results suggest correlations between melt timing and wildfire occurrence spatially and temporally, there are many other factors that affect both phenomena, thus the analyses should not be viewed as an attempt to determine cause and effect. In essence, both variables are responding to similar climatic forcing depending upon the magnitude of the effects seasonally. Snow cover heterogeneity is governed by climate, land cover, and topography with temperature, precipitation, radiation, elevation, slope, and aspect serving as key controls on its distribution and persistence (Tong *et al*., 2009). Fire occurrence and spread in the boreal forest is largely controlled by climate (air temperature, rainfall, humidity, and wind speed), circulation patterns (Skinner *et al*., 2006), fuel abundance, and moisture of the organic soil layer (a result of precipitation and thawing permafrost) (Kasischke *et al*., 2002).

Furthermore, El Niño events creating warmer and drier conditions in Alaska coincide with high fire years (Hess *et al*., 2001) and alter snowmelt patterns, providing evidence that large-scale atmospheric and long-term climatic patterns greatly affect both variables. Large-scale sea surface temperatures and Pacific Ocean processes (ENSO/PDO) have been found to largely explain Canadian fire severity with the warm ENSO phase and positive PDO phase creating dry conditions and high fire years (Skinner *et al*., 2006). Pacific Ocean sea surface temperature anomalies were found to correlate with fire activity in British Columbia (Wang *et al*., 2010). Additionally, the increase in burned areas in Canada has been attributed to mid-tropospheric circulation anomalies at 500 hPa heights, with more meridional circulation and strong, northerly displaced ridging producing anomalous dry, warm conditions that fuel fires (Skinner *et al*., 1999).

CONCLUSIONS

Investigation of two high fire years and two low fire years in the Porcupine River basin suggest there are correlations between fire occurrence, melt onset and end of melt-refreeze date. Areas affected by fire tend to have had earlier melt onset and end of melt-refreeze. This is supported by comparison between pixels, comparison between high and low fire years, and in the change to later melt onset and end melt-refreeze dates in years following fires. In remote, snowmelt dominated basins, such as the Porcupine, that lack sufficient meteorological and hydrometric instrumentation, passive microwave remote sensing may be useful in determining areas prone to fire potential later in the year by examining melt timing (particularly end of melt-refreeze) dates. Previous studies have found a weak correlation between number of fires in Alaska and drought indices usually used to predict fire danger, and seasonal forecasts of upcoming fire seasons lack skill (Wendler *et al.,* 2010). Further work is necessary to determine the potential utility of remotely sensed snowmelt timing estimates in improving such seasonal fire forecasting. In addition, such information may serve in modeling snowmelt runoff and peak discharge as overland flow is known to increase significantly for areas affected by wildfire.

ACKNOWLEDGEMENTS

The authors kindly thank the National Snow and Ice Data Center for providing AMSR-E and MODIS data and Environment Canada for the meteorological and hydrometric data. This research was conducted with the support of a NASA Earth and Space Science Fellowship.

REFERENCES

Apgar JD, Ramage JM, McKenney RA, and Maltais P. 2007. Preliminary AMSR-E Algorithm for Snowmelt Onset Detection in Subarctic Heterogeneous Terrain, *Hydrological Processes* **21**: 1587−1596. DOI: 10.1002/hyp.6721.

Ashcroft P, and Wentz F. 2006. Updated daily. *AMSR-E/Aqua L2A Global Swath Spatially-Resampled Brightness Temperatures V002*, [2004−2007]. Boulder, Colorado USA: National Snow and Ice Data Center. Digital media.

Balshi MS, McGuire AD, Duffy P, Flannigan M, Kicklighter DW,and Melillo J. 2009. Vulnerability of carbon storage in North American boreal forests to wildfires during the 21st century. *Global Change Biology* **15**: 1491−1510. DOI:10.1111/j.1365-2486.2009.01877.x.

Berrisford P, Dee D, Fielding K, Fuentes M, Kallberg P, Kobayashi S, and Uppala S. 2009. The ERA-Interim archive *ERA Report Series* 1. European Centre for Medium Range Weather Forecasts, UK.

Brabets TP, and Long D. 2002. Coverage YUK_LAND NASQAN Yukon River Basin, Canada, and Alaska Landcover. Map. USGS: Anchorage, AK.A <http://agdc.usgs.gov/data/usgs/water/metadata/yuk_land.html>

Brabets TP, Wang B, and Meade RH. 2000. Environmental and hydrologic overview of the Yukon River Basin, Alaska and Canada. *USGS Water-Resources Investigations Report 99-4204*. Anchorage, Alaska.

Burn CR. 1998. The response (1958−1997) of permafrost and near-surface ground temperatures to forest fire, Takhini River valley, southern Yukon Territory. *Canadian Journal of Earth Sciences* **35(2)**: 184−199. DOI: 10.1139/e97-105.

Chang TC, Gloersen P, Schmugge T, Wilheit TT, and Zwally HJ. 1976. Microwave emission from snow and glacier ice. *Journal of Glaciology* **16(74)**: 23−39.

Gillett NP, Weaver AJ, Zwiers FW, and Flannigan MD. 2004. Detecting the effect of climate change on Canadian forest fires. *Geophysical Research Letters* **31**: L18211. DOI: 10.1029/2004GL020876.

Hall DK, Sturm M, Benson CS, Chang ATC, Foster JL, Garbeil H, and Chacho E. 1991. Passive microwave remote and *in situ* measurements of arctic and subarctic snow covers in Alaska. *Remote Sensing of Environment* **38**: 161−172. DOI: 10.1016/0034-4257(91)90086-L.

Hess JC, Scott CA, Hufford GL, and Fleming MD. 2001. El Nino and its impact on fire weather conditions in Alaska. *International Journal of Wildland Fire* **10**: 1−13. DOI: 10.1071/WF01007.

Kasischke ES, Rupp TS, and Verbyla DL. 2006. Fire trends in the Alaskan Boreal Forest. Chapter 17 in *Alaska's Changing Boreal Forest*. Eds. Chapin III FS, Oswood MW, Cleve KV, and Viereck LA, Verbyla DL. Oxford Press.

Kasischke ES, and Turetsky MR. 2006. Recent changes in the fire regime across the North American boreal region—spatial and temporal patterns of burning across Canada and Alaska. *Geophysical Research Letters* **33**: L09703. DOI: 10.1029/2006GL025677.

Kasischke ES, Verbyla DL, Rupp TS, McGuire AD, Murphy KA, Jandt R, Barnes JL, Hoy EE, Duffy PA, Calef M, and Turetsky MR. 2010. Alaska's changing fire regime—implications for the vulnerability of boreal forests. *Can. J. For. Res*. **40**: 1313−24. DOI: 10.1139/X10-098.

Kasischke ES, Williams D, and Barry D. 2002. Analysis of the patterns of large fires in the boreal forest region of Alaska. *International Journal of Wildland Fire* **11**: 131−144. DOI:10.1071/WF02023.

Pomeroy JW, Gray DM, Hedstrom NR, and Janowicz JR. 2002. Prediction of seasonal snow accumulation in cold climate forests. *Hydrological Processes* **16(18)**: 3543−3558. DOI: 10.1002/hyp.1228.

Ramage JM, McKenney RA, Thorson B, Maltais P, and Kopczynski SE. 2006. Relationship between Passive Microwave-Derived Snowmelt & Surface-Measured Discharge, Wheaton R., Yukon, *Hydrological Processes* **20**: 689−704. DOI: 10.1002/hyp.6133.

Randerson JT, Lui H, Flanner MG, Chambers SD, Jin Y, Hess PG, Pfister G, Mack MC, Treseder KK, Welp LR, Chapin FS, Harden JW, Goulden ML, Lyons E, Neff JC, Schuur EAG, and Zender CS. 2006. The impact of boreal forest fire on climate warming. *Science* **314**: 1130−1132. DOI:10.1126/science.1132075.

Seibert J, McDonnell JJ, and Woodsmith RD. 2010. Effects of wildfire on catchment runoff response: a modeling approach to detect changes in snow-dominated forested catchments. *Hydrology Research* **41.5**: 378−390. DOI: 10.2166/nh.2010.036.

Shakesby RA, and Doerr SH. 2006. Wildlife as a hydrological and geomorphological agent. *Earth-Science Reviews* **74**: 269−307. DOI: 10.1016/j.earscirev.2005.10.006.

Shenoy A, Johnstone JF, Kasischke ES, and Kielland K. 2011. Persistent effects of fire severity on early successional forests in interior Alaska. *Forest Ecology and Management* **261**: 381−390. DOI: 10.1016/j.foreco.2010.10.021.

Skinner WR, Shabbar A, Flannigan MD, and Logan K. 2006. Large forest fires in Canada and the relationship to global sea surface temperatures. *Journal of Geophysical Research* **111**: D14106. DOI: 10.1029/2005JD006738.

Skinner WR, Stocks BJ, Martell DL, Bonsal B, and Shabbar A. 1999. The association between circulation anomalies in the mid-troposphere and area burned by wildland fire in Canada. *Theoretical and Applied Climatology* **63**: 89−105. DOI: 10.1007/s007040050095.

Stocks BJ, Mason JA, Todd JB, Bosch EM, Wotton BM, Amiro BD, Flannigan MD, Hirsch KG, Logan KA, Martell DL, and Skinner WR. 2002. Large forest fires in Canada, 1959−1997. *J. of Geophysical Research* **107**: 8149. DOI: 10.1029/2001JD000484.

Tong J, Dery SJ, and Jackson PL. 2009. Topographic control of snow distribution in an alpine watershed of western Canada inferred from spatially-filtered MODIS snow products. *Hydrology and Earth System Sciences* **13**: 319−326. DOI: www.hydrol-earth-syst-sci.net/13/319/2009/.

Turetsky MR, Kane ES, Harden JW, Ottmar RD, Manies KL, Hoy E, and Kasischke ES. 2010. Recent acceleration of biomass burning and carbon losses in Alaskan forests and peatlands. *Nature Geoscience* **4**: 27−31. DOI: 10.1038/ngeo1027.

Ulaby FT, Moore RK, and Fung AK. 1986. *Microwave Remote Sensing: Active and Passive, Vol. III: From Theory to Applications*. Artech House: Dedham.

USDA Forest Service Remote Sensing Applications Center (RSAC). 2010. 2003−2010 MODIS MCD14ML Collection 5, Version 1 (Alaska). Vector Digital Data.

Wang Y, Flannigan M, and Anderson K. 2010. Correlations between forest fires in British Columbia, Canada, and sea surface temperature of the Pacific Ocean. *Ecological Modelling* **221(1)**: 122−129. DOI: 10.1016/j.ecolmodel.2008.12.007.

Wendler G, Conner J, Moore B, Shulski M, and Stuefer M. 2010. Climatology of Alaskan wildfires with special emphasis on the extreme year of 2004. *Theoretical and Applied Climatology*. DOI: 10.1007/s00704-010-0357-9.